



ELSEVIER

Available online at www.sciencedirect.com

SCIENCE @ DIRECT®

International Journal of Impact Engineering 32 (2006) 947–967

INTERNATIONAL
JOURNAL OF
IMPACT
ENGINEERING

www.elsevier.com/locate/ijimpeng

Shear band spacing in thermoviscoplastic materials

R.C. Batra*, Z.G. Wei

Department of Engineering Science and Mechanics, MC 0219, Virginia Polytechnic Institute and State University, Blacksburg, VA 24061, USA

Received 1 March 2004; accepted 10 August 2004

Available online 6 October 2004

Abstract

A closed-form expression for shear band spacing in strain-hardening, strain-rate-hardening and thermally softening thermoviscoplastic materials is derived by studying the stability of a homogeneous solution of equations governing its simple shearing deformations. The wavelength of the perturbation that maximizes its initial growth rate is assumed to determine the shear band spacing, L_s . The dependence of L_s upon various material parameters and the nominal strain rate, $\dot{\epsilon}$, is delineated. When written as $L_s = A_1 k^{\chi_1}$ or $A_2 \dot{\epsilon}^{\chi_2}$ where A_1 and A_2 are parameters and k is the thermal conductivity, it is found that $\chi_2 \simeq -0.787$ and χ_1 depends upon the strain-rate hardening exponent m ; $\chi_1 \simeq 0.5$ for $m \simeq 10^{-6}$ and $n \simeq 0.011$, decreases rapidly to 0.21 for $m \simeq 10^{-4}$ and $n \simeq 0.011$, and then increases slowly to 0.25 for $m \simeq 0.05$ and $n \simeq 0.011$. However, for $m = 0$ and $n \neq 0$, $\chi_1 = 1$.

© 2004 Elsevier Ltd. All rights reserved.

Keywords: Simple shearing; Perturbation method; Analytical expression

1. Introduction

The study of adiabatic shear bands (ASBs) is important since they precede ductile failure in most materials deformed at high strain rates. An ASB is a narrow region, usually a few micrometers wide, with plastic strains often exceeding 1. Even though Tresca [1] observed these in 1880, research in this area intensified with the work of Zener and Hollomon [2] who not only

*Corresponding author. Tel.: +1-540-2316051; fax: +1-540-2314574.

E-mail addresses: rbatra@vt.edu (R.C. Batra), zwei@vt.edu (Z.G. Wei).

observed ASBs during the punching of a hole in a low carbon steel plate but also postulated that they initiate when a material point becomes unstable due to softening caused by heating overcoming its hardening induced by strain and strain-rate effects.

The perturbation technique to analyze the stability of transient simple shearing deformations of a thermoviscoplastic body has been employed by Bai [3]. A homogeneous solution of the problem at time t_0 is perturbed by an infinitesimal amount and governing equations are linearized with coefficients evaluated at time t_0 . Bai [3] derived conditions necessary for the homogeneous solution to become unstable and also computed the wavelength of the perturbation that maximized its initial growth rate; he defined a characteristic length in terms of this wavelength. This and other works are summarized in books by Bai and Dodd [4] and Wright [5], in the review article of Tomita [6], and in books or special issues of journals edited by Zbib et al. [7], Armstrong et al. [8], Perzyna [9], Batra and Zbib [10] and Batra et al. [11]. Batra and Chen [12] have pointed out that for locally adiabatic simple shearing deformations of a thermoviscoplastic body, the critical strain evaluated from Bai's criterion equals that given by the Considère condition [13] which states that a structure becomes unstable when the load required to deform it is maximum. For the simple shearing problem, the Considère criterion is equivalent to the shear stress attaining its maximum value. Batra and Kim [14] have shown through numerical experiments that the thermal conductivity has a negligible influence on the time of initiation of an ASB but affects the post-localization process. Thus, even when heat conduction is considered, the critical strain computed from Bai's instability criterion agrees with that from the Considère condition. Wei and Batra [15] have shown that this holds even when damage evolution is also considered mainly because not much damage has evolved till the time of initiation of an ASB.

Wright and Ockendon [16] also examined the growth of infinitesimal perturbations superimposed upon a homogeneous solution and ignored strain-hardening effects. They postulated that, in an infinite body, perturbations growing at different sites will not merge and result in multiple ASBs. They equated the shear band spacing to the wavelength of the instability mode that maximizes the initial growth rate of infinitesimal perturbations. The shear band spacing so determined can be related to Bai's [3] characteristic length. For materials obeying the constitutive relation $\sigma = \sigma_0(1 - \alpha(\theta - \theta_0))(\dot{\gamma}/\dot{\gamma}_0)^m$, Wright and Ockendon's expression for the shear band spacing is $L_{WO} = 2\pi(m^3kc/(\dot{\gamma}^3\alpha^2\sigma_0))^{1/4}$. Here σ is the shear stress, γ the shear strain within the ASB, α the thermal softening coefficient, m the strain-rate-hardening exponent, θ the present temperature within the ASB, c the specific heat, k the thermal conductivity and $\dot{\gamma}_0$ the nominal strain rate. Values of $\dot{\gamma}$ and θ in an ASB need to be estimated in order to compute L_{WO} . Molinari [17] considered strain hardening effects and defined the shear band spacing as $L_M = \inf_{t_0 \geq 0} 2\pi/\xi_m(t_0)$, where ξ_m is the wavelength of the perturbation introduced at time t_0 that has the maximum growth rate at t_0 . For materials obeying the constitutive relation $\dot{\gamma} = \mu_0^{-1/m}\sigma^{1/m}(\gamma + \gamma_i)^{-n/m}\theta^{-v/m}$, Molinari's approximate expression for the shear band spacing is

$$\begin{aligned} L_M &= L_0(1 + (3\rho c\partial\dot{\gamma}/\partial\gamma)(4\beta\sigma^0\partial\dot{\gamma}/\partial\theta))^{-1} \\ &= 2\pi((m^3kc(\theta^0)^2/(\beta^2\dot{\gamma}^3v^2\sigma^0(1+m)))^{1/4} \left(1 + \frac{3\rho cn}{4\beta v\sigma^0} \frac{\theta^0}{\gamma + \gamma_i}\right)^{-1}, \end{aligned}$$

where L_0 is the shear band spacing for $n = 0$, σ^0 the shear stress and θ^0 the temperature at time t_0 in the homogeneous solution, β the fraction of plastic working converted into heating, and ρ the

mass density. Note that Bai [3] and Wright and Ockendon [16] did not find the infimum of $2\pi/\xi_m(t_0)$. In contrast to the perturbation method, Grady and Kipp [18] studied simple shearing deformations of a thermally softening rigid plastic material and considered the momentum diffusion due to unloading within an ASB to find the shear band spacing. Based on the constitutive relation $\sigma = \sigma_0(1 - \alpha(\theta - \theta_0))$, Grady and Kipp’s expression for the shear band spacing is $L_{GK} = 2(9kc/(\dot{\gamma}^3\alpha^2\sigma_0))^{1/4}$. We note that the dependence of L_{WO} and L_{GK} upon $k, c, \dot{\gamma}, \alpha$ and σ_0 is the same. However, L_{GK} cannot be deduced from L_{WO} since $L_{WO} = 0$ for $m = 0$. Batra and Chen [19] considered the effects of strain-rate gradients in strain-rate hardening and thermally softening materials. Three viscoplastic relations, namely those due to Wright and Batra (e.g. see [19]), power law and Johnson–Cook [20] were considered. For locally adiabatic deformations (i.e. $k = 0$), they found that

$$L_{BC} = \begin{cases} \left(\frac{\ell}{\dot{\gamma}_0}\right)^{1/2} \left(\frac{m(1 - \alpha\theta_0)c}{\alpha}\right)^{1/4} & \text{for the Wright–Batra relation,} \\ \left(\frac{\ell}{\dot{\gamma}_0}\right)^{1/2} \left(-\frac{c\theta_i m}{v}\right)^{1/4} & \text{for the power law,} \\ \left(\frac{\ell}{\dot{\gamma}_0}\right)^{1/2} \left[\frac{cC(1 - \alpha\theta_0)}{\alpha(1 + C \ln \dot{\gamma}_0)}\right]^{1/4} & \text{for the Johnson–Cook relation,} \end{cases}$$

where ℓ is a material characteristic length, C defines strain-rate hardening of the material in the Johnson–Cook relation, and θ_i is the temperature when the homogeneous solution is perturbed. For heat-conducting nonpolar materials they found that

$$\tilde{L}_{BC} = \begin{cases} \left(\frac{m^3kc(1 - \alpha\theta_0)}{(1 + m)\dot{\gamma}_0^3\alpha^2\sigma_0}\right)^{1/4} & \text{for the Wright–Batra relation,} \\ \left(\frac{m^3\theta_0^2kc}{(1 + m)\dot{\gamma}_0^3\sigma_0v^2}\right)^{1/4} & \text{for the power law,} \\ \left(\frac{C^3kc(1 - \alpha\theta_0)}{\alpha^2\dot{\gamma}_0^3(1 + C \ln \dot{\gamma}_0)^3\sigma_0}\right)^{1/4} & \text{for the Johnson–Cook relation.} \end{cases}$$

Thus for positive shear band spacing, either the thermal conductivity or the material characteristic length must be positive. Chen and Batra [21] have also analyzed numerically the shear band spacing in strain-hardening, strain-rate hardening and thermally softening strain-rate gradient-dependent materials. For locally adiabatic deformations of a material obeying the constitutive relation of the type used by Molinari but generalized to strain-rate gradient-dependent materials, they found the following expression for the shear band spacing:

$$L_{CB} = 2\pi(\ell/\dot{\gamma}_0)^{1/2} \left(\frac{mc\theta_0}{(1 - (-v\tilde{n}))^{-1/2}}\right)^{1/4} (-v)^{-1/8} [(-v)^{1/2} - (\tilde{n})^{1/2}]^{-1/4}.$$

Here $\tilde{n} = n/(1 + n)$, and θ_0 is the temperature when the homogeneous solution is perturbed. For $n \ll 1$, $\tilde{n} = n$. For L_{CB} to be positive, $1 > (-v\tilde{n})^{-1/2}$ and $|v| > \tilde{n}$; these inequalities hold for most

materials. We note that L_{WO} and \tilde{L}_{BC} are proportional to $m^{3/4}$ but L_{BC} is proportional to $m^{1/4}$. However, the dependence of L_{M} and L_{CB} upon the strain-hardening exponent n is more involved.

Nesterenko et al. [22] and Xue et al. [23] observed multiple shear bands, generally 1 mm apart, during the radial collapse of explosively loaded thick-walled titanium and stainless steel hollow cylinders. The average strain rate within the shear-banded region was estimated to be $10^4/\text{s}$.

In addition to thermal softening, strain hardening and strain-rate hardening, the softening due to accumulated damage because of the nucleation and growth of voids may also influence shear band spacing. Wei and Batra [15] have shown that the damage evolution decreases the instability strain.

We note that the aforementioned studies have not derived a closed-form expression for the shear band spacing for strain- and strain-rate hardening but thermally softening materials. Here we obtain a closed form expression for the shear band spacing. Even though we consider infinitesimal perturbations that identically satisfy boundary conditions, the need to differentiate expressions with respect to the wavelength of admissible perturbations requires that the specimen thickness be very large as compared to the wavelengths considered. It is found that effects of the thermal conductivity and the strain-rate hardening on the shear band spacing are more strongly coupled than previously recognized.

2. Formulation of the problem

We study simple shearing deformations of an isotropic, homogeneous, strain hardening, strain-rate hardening and thermally softening thermoviscoplastic body occupying the region $0 \leq x \leq h$ and sheared in the y -direction. Equations governing its thermomechanical deformations are

$$\rho \dot{v} = \sigma_{,x}, \quad (1)$$

$$\dot{\varepsilon} = v_{,x}, \quad (2)$$

$$\rho c \dot{\theta} = \beta \sigma \dot{\varepsilon} + k \theta_{,xx}, \quad (3)$$

where ρ is the mass density, v the velocity of a material particle in the direction of shearing, σ the shear stress, ε the shear strain, c the specific heat, θ the temperature rise, β the fraction of plastic working converted into heating or the Taylor–Quinney parameter, and k the thermal conductivity, a superimposed dot indicates the material time derivative which for this problem equals the partial derivative with respect to time t , and $v_{,x} = \partial v / \partial x$. In Eq. (3) we have employed Fourier's law of heat conduction, and neglected elastic deformations which is reasonable because plastic deformations envisaged are large as compared to the elastic deformations. The flow stress σ of the thermoviscoplastic material is given by

$$\sigma = \sigma(\varepsilon, \dot{\varepsilon}, \theta). \quad (4)$$

Initial conditions are not needed since we will study the stability of a homogeneous solution of the problem. The following two sets of boundary conditions are considered. Either

$$\begin{aligned} v(0, t) = 0, \quad v(h, t) = v_0, \\ \theta_{,x}(0, t) = 0, \quad \theta_{,x}(h, t) = 0, \end{aligned} \quad (5)$$

or

$$\begin{aligned} \sigma(0, t) &= \sigma(h, t) = \bar{\sigma}(t), \\ \theta(0, t) &= \theta(h, t) = \bar{\theta}(t). \end{aligned} \tag{6}$$

That is, either the shearing speed is prescribed on the two thermally insulated bounding surfaces or they are sheared with equal and opposite tractions and are held at the same time-dependent temperature. For these two sets of boundary conditions, the commonly considered spatially periodic perturbations satisfy exactly the prescribed boundary conditions.

3. Analysis of material instability

Except for the fact that perturbations considered here satisfy boundary condition (5) or (6), the analysis presented in this section is borrowed from Bai [3] and is included for the sake of completeness. A similar approach has been adopted by Wright and Ockendon [16], Molinari [17], Batra and Chen [19] and Chen and Batra [21].

Let $\mathbf{S}^0(t) \equiv (\varepsilon^0(t), \sigma^0(t), \theta^0(t))$ be a steady-state solution of either one of the two boundary-value problems, and $\delta\mathbf{S}(t_0, x, t)$ with $|\delta\mathbf{S}(t_0, x, t)| \ll |\mathbf{S}(x, t_0)|$ denote an infinitesimal perturbation in $\mathbf{S}^0(t_0)$. Perturbations considered are such that $\mathbf{S}^0(t_0) + \delta\mathbf{S}(t_0, x, t)$ satisfies the prescribed boundary conditions. Thus, either

$$\delta v(0, t) = \delta v(h, t) = \delta\theta_{,x}(0, t) = \delta\theta_{,x}(h, t) = 0 \tag{7}$$

or

$$\delta\sigma(0, t) = \delta\sigma(h, t) = \delta\theta(0, t) = \delta\theta(h, t) = 0, \tag{8}$$

which follow from Eqs. (5) and (6), respectively. Eqs. (7)₁, (7)₂ and (1) imply that

$$\delta\sigma_{,x}(0, t) = \delta\sigma_{,x}(h, t) = 0. \tag{9}$$

The admissible perturbation field for boundary conditions (5) is

$$\delta\mathbf{S} = \delta\mathbf{S}^0 \cos \xi x e^{\eta(t-t_0)}, \quad \xi = \frac{2\tilde{m}\pi}{h}, \tag{10}$$

and that for boundary conditions (6) is

$$\delta\mathbf{S} = \delta\mathbf{S}^0 \sin \xi x e^{\eta(t-t_0)}, \quad \xi = \frac{2\tilde{m}\pi}{h}, \tag{11}$$

where $\delta\mathbf{S}^0$ is the amplitude of the perturbation, ξ the wavenumber, \tilde{m} an integer, and η equals the growth rate of the perturbation at time t_0 . $\text{Re}(\eta) > 0$ implies that perturbations will grow signifying the instability of the homogeneous solution at time t_0 ; otherwise it is stable. The admissible wavelengths in perturbations (10) and (11) can have discrete values determined by the values of h and \tilde{m} . Assuming that these wavelengths are much smaller than h , we will treat ξ as a continuous variable. For an infinite body, this condition is trivially satisfied.

Eq. (4) gives

$$\delta\sigma = (Q_0 + \eta R_0)\delta\varepsilon - P_0\delta\theta, \tag{12}$$

where

$$P_0 = -\frac{\partial \sigma}{\partial \theta} \Big|_{\mathbf{S}=\mathbf{S}^0}, \quad Q_0 = \frac{\partial \sigma}{\partial \varepsilon} \Big|_{\mathbf{S}=\mathbf{S}^0}, \quad R_0 = \frac{\partial \sigma}{\partial \dot{\varepsilon}} \Big|_{\mathbf{S}=\mathbf{S}^0}. \tag{13}$$

Thus P_0 equals thermal softening of the material, Q_0 its strain hardening, and R_0 strain-rate hardening. Note that

$$P_0 \geq 0, \quad Q_0 \geq 0 \quad \text{and} \quad R_0 \geq 0. \tag{14}$$

Substitution of $\mathbf{S} = \mathbf{S}^0 + \delta \mathbf{S}$ in Eqs. (1)–(4), linearizing the resulting equations in $\delta \mathbf{S}^0$, and requiring that the system of simultaneous linear equations have a nontrivial solution, we obtain the following equation for η :

$$\bar{\eta}^3 + a_1 \bar{\eta}^2 + a_2 \bar{\eta} + \bar{\xi}^4 = 0, \tag{15}$$

where

$$\begin{aligned} \bar{\eta} &= \frac{k\eta}{cQ_0}, \quad \bar{\xi} = \frac{k\xi}{c\sqrt{\rho Q_0}}, \quad a_1(\bar{\xi}, \varepsilon^0) = \Gamma + (1 + I)\bar{\xi}^2, \\ a_2(\bar{\xi}, \varepsilon^0) &= (I\bar{\xi}^2 + 1 - J)\bar{\xi}^2, \\ I &= \frac{cR_0}{k}, \quad J = \frac{\beta\sigma^0 P_0}{\rho c Q_0}, \quad \Gamma = \frac{\beta k P_0 \dot{\varepsilon}^0}{\rho c^2 Q_0}. \end{aligned} \tag{16}$$

For every short wavelengths, $\bar{\xi} \rightarrow \infty$, Eq. (15) has the solution $\bar{\eta} = -1/I$, which is negative. For extremely long wavelengths, $\bar{\xi} \rightarrow 0$, $\bar{\eta} = -\Gamma$ and 0. If $\bar{\eta} \rightarrow 0$ from above, then the simple shearing deformation is unstable for perturbations of very long wavelengths, and the growth rate of the perturbed solution decreases with an increase in the wavelength of perturbations. Thus the simple shearing deformation is stable with respect to disturbances of infinitesimal wavelengths, but may be unstable with respect to disturbances of finite wavelengths.

For given t_0 and $\bar{\xi}$, the root of Eq. (15) with the largest positive real part will make the homogeneous solution $\mathbf{S}^0(t)$ most unstable. Numerical experiments have shown that η is real for perturbations introduced after the shear stress has peaked. We seek the value $\bar{\xi}_m$ of $\bar{\xi}$ for which $\bar{\eta}$ has the maximum value $\bar{\eta}_m$; $\bar{\eta}_m$ and $\bar{\xi}_m$ satisfy Eq. (15) and

$$\frac{d\bar{\eta}}{d\bar{\xi}} \Big|_{(\bar{\eta}=\bar{\eta}_m, \bar{\xi}=\bar{\xi}_m)} = 0. \tag{17}$$

Eqs. (15) and (17) give

$$\bar{\xi}_m^2 = \bar{\eta}_m \frac{(J - 1) - (1 + I)\bar{\eta}_m}{2(I\bar{\eta}_m + 1)}. \tag{18}$$

Since $\bar{\xi}_m^2 > 0$, therefore,

$$0 < \bar{\eta}_m \leq \frac{J - 1}{1 + I}. \tag{19}$$

Substitution for $\bar{\xi}_m^2$ from Eq. (18) into Eq. (15) yields

$$4(1 + I\bar{\eta}_m)(\Gamma + \bar{\eta}_m) = [(J - 1) - (1 + I)\bar{\eta}_m]^2. \tag{20}$$

Following Bai's [3] reasoning, the instability condition is

$$J > 1 + 2\sqrt{I} \quad (21)$$

or

$$\frac{\beta\sigma^0 P_0}{\rho c Q_0} > 1 + 2 \left[\frac{\beta k P_0 \dot{\epsilon}^0}{\rho c^2 Q_0} \right]^{1/2}. \quad (22)$$

For locally adiabatic deformations, $k = 0$, and the instability criterion (22) simplifies to

$$\frac{\beta\sigma^0 P_0}{\rho c Q_0} > 1. \quad (23)$$

Thus the material becomes unstable when the softening due to heating exceeds its strain hardening. Even though the strain-rate hardening does not explicitly appear in the instability criterion (22) or (23) it influences σ^0 , P_0 and Q_0 . In the presence of heat conduction, higher values of $\dot{\epsilon}^0$ delay the onset of instability.

Batra and Chen [12] and Wei and Batra [15] have shown that the instability criterion (23) is equivalent to the Considère [13] criterion which for the simple shearing problem reduces to σ being maximum at the instant the material becomes unstable.

4. Shear band spacing

Wright and Ockendon [16] have proposed that the spacing, L_s , between two adjacent shear bands is given by

$$L_s = 2\pi/\bar{\xi}_m(t_0), \quad (24)$$

where $\bar{\xi}_m(t_0)$ is the wavenumber, in units of 1/length, corresponding to the maximum growth rate $\bar{\eta}_m$ of perturbations at time t_0 of the homogeneous solution $\mathbf{S}^0(t)$ of Eqs. (3) and (8). $\bar{\eta}_m$ and $\bar{\xi}_m$ satisfy (18). Numerical experiments of Batra [26], Batra and Kim [27], and Kwon and Batra [28] tend to support this hypothesis for simple materials but not for strain-rate gradient-dependent materials. They disturbed the homogeneous solution by introducing a finite size temperature perturbation with multiple cusps and numerically solved the resulting nonlinear problem. Kwon and Batra [28] found that, for simple materials an ASB formed at each trough in the cosine wave in the specimen deformed at an average strain-rate $\dot{\epsilon}_0$ of 500 s^{-1} but at each crest when $\dot{\epsilon}_0 = 50,000 \text{ s}^{-1}$. For strain-rate gradient-dependent materials with material characteristic length equal to 0.5% of the specimen thickness, an ASB formed at each of the two bounding surfaces when the shearing speed was prescribed to give $\dot{\epsilon}_0 = 500 \text{ s}^{-1}$, and multiple ASBs formed at each crest when $\dot{\epsilon}_0 = 50,000 \text{ s}^{-1}$. These authors considered finite size perturbations satisfying boundary conditions in a specimen of thickness h . They did not investigate the dependence of results upon the finite element mesh. Numerical results presented in [12,19,21] reveal that the wavelength of the perturbation corresponding to the maximum growth rate depends upon the strain level of the perturbed homogeneous deformation.

From Eqs. (15) and (17), or alternatively from Eq. (18) we get

$$a_4 \bar{\eta}_m^2 + a_5 \bar{\eta}_m + a_6 = 0, \quad (25)$$

where

$$a_4 = 1 + I, \quad a_5 = 2I\bar{\xi}^2 + (1 - J), \quad a_6 = 2\bar{\xi}^2. \quad (26)$$

Eqs. (15) and (25) when solved simultaneously for $\bar{\eta}_m$ and $\bar{\xi}_m$ give

$$\begin{aligned} \bar{\eta}_m &= \frac{a_6(a_1 a_4 - a_5) - a_4^2 \bar{\xi}^4}{a_4(a_2 a_4 - a_6) - a_5(a_1 a_4 - a_5)}, \\ &= \frac{\bar{\xi}^2 \{(1 - I)^2 \bar{\xi}^2 + 2\Gamma(1 + I) - 2(1 - J)\}}{-I(1 - I)^2 \bar{\xi}^4 + 2\bar{\xi}^2 [2I(1 - J) - (1 + I)(1 + I\Gamma)] + (1 - J)[(1 - J) - \Gamma(1 + I)]}. \end{aligned} \quad (27)$$

Upon substitution from Eq. (27) into Eq. (25) we obtain

$$b_2 \bar{\xi}_m^4 + b_3 \bar{\xi}_m^2 + b_4 = 0, \quad (28)$$

where

$$\begin{aligned} b_2 &= (1 - I)^2 [1 + IJ], \\ b_3 &= 2[2I(1 - J)^2 - (1 + I)(1 - J)(3 + I\Gamma) + 2(\Gamma(1 + I^2) + 2)], \\ b_4 &= (4\Gamma - (1 - J)^2)[\Gamma(1 + I) - (1 - J)]. \end{aligned} \quad (29)$$

A positive root of Eq. (28) is

$$\bar{\xi}_m^2 = \frac{-b_3 + \sqrt{b_3^2 - 4b_2 b_4}}{2b_2}. \quad (30)$$

Substitution from Eqs. (30) and (16)₂ into (24) gives the shear band spacing for a thermoviscoplastic material deformed in simple shear. The complexity of the expression makes it difficult to interpret how various factors influence L_s . However, for negligible strain-rate hardening or very high strain-rate hardening, Eq. (30) can be simplified.

For a strain-rate independent material, $R_0 = 0$, $I = 0$, and Eq. (30) with substitutions from Eq. (29) reduces to

$$\bar{\xi}_m^2 = -(1 + 2\Gamma + 3M) + (3 + M)(M + \Gamma)^{1/2}, \quad (31)$$

where

$$M = \frac{\beta \sigma^0 P_0}{\rho c Q_0}. \quad (32)$$

For most materials deformed at high strain rates

$$\Gamma = \frac{\beta k P_0 \dot{\epsilon}^0}{\rho c^2 Q_0} = M \frac{k \dot{\epsilon}^0}{c \sigma^0} \ll M, \quad (33)$$

in which case Eq. (31) can be approximated by

$$\bar{\xi}_m^2 \simeq -(1 + 3M) + (3 + M)\sqrt{M}. \tag{34}$$

For many materials, $\beta\sigma^0/(\rho c) \simeq O(10^2)$, and $M \gg 1$. Then $\bar{\xi}_m \simeq M^{3/4}$ and

$$L_s \simeq 2\pi k\beta^{-3/4} \left(\frac{\rho}{c}\right)^{1/4} \left(\frac{Q_0}{(\sigma^0 P_0)^3}\right)^{1/4}. \tag{35}$$

Thus for a non-strain-rate hardening material, $L_s \sim k$, $L_s \sim \rho^{1/4}$, $L_s \sim c^{-1/4}$, $L_s \sim Q_0^{1/4}$ and $L_s \sim (\sigma^0 P_0)^{-3/4}$. A higher value of the strain-hardening enlarges the shear band spacing but higher values of the shear stress and the thermal softening reduce the spacing between adjacent shear bands. For the constitutive relation used by Molinari [17] and given in the Introduction,

$$L_s = 2\pi k\beta^{-3/4} \left(\frac{\rho}{c}\right)^{1/4} \left(-\frac{n}{\mu_0^5 v^3}\right)^{1/4} (\gamma^0 + \gamma_i)^{-(5n+1)/4} (\theta^0)^{(-5v+3)/4}. \tag{36}$$

For the constitutive relation

$$\sigma = \sigma_0 \left(1 + \frac{\varepsilon}{\varepsilon_y}\right)^n \left(\frac{\theta_m - \theta}{\theta_m - \theta_r}\right)^v, \quad v > 0$$

employed by Wright and Batra

$$L_s = 2\pi k\beta^{-3/4} \left(\frac{\rho}{c}\right)^{1/4} \left(\frac{n(\theta_m - \theta_r)^3}{\sigma_0^5 v^3 \varepsilon_y}\right)^{1/4} \left(1 + \frac{\varepsilon^0}{\varepsilon_y}\right)^{-(5n+1)/4} \left(\frac{\theta_m - \theta^0}{\theta_m - \theta_r}\right)^{(-5v+3)/4}. \tag{37}$$

Here θ_m and θ_r are, respectively, the melting temperature of the material and the room temperature. The strain hardening exponent, n , appears in two terms, one of which implies that L_s increases with an increase in the value of n but the other has the opposite effect. Thus it is hard to delineate the effect of n on the shear band spacing from expressions (36) and (37).

For a strongly strain-rate hardening material, $R_0 \rightarrow \infty$, $I \rightarrow \infty$ and

$$\frac{d\bar{\eta}}{d\bar{\xi}^2} = -\frac{I\bar{\eta}^2 + 2(I\bar{\eta} + \bar{\xi}^2)}{3\bar{\eta}^2 + I(2\bar{\eta} + \bar{\xi}^2)\bar{\xi}^2} < 0. \tag{38}$$

That is, the initial growth rate of a perturbation increases with a decrease in the wavelength of the perturbation. Hence $L_s \rightarrow \infty$ as $R_0 \rightarrow \infty$.

Expression (35) and that obtained by substituting from Eqs. (30) and (16)₂ into Eq. (24) for the shear band spacing cannot be compared with those of Wright and Ockendon [16] and Grady and Kipp [17] since they neglected strain hardening effects. Here, the strain-hardening parameter Q_0 appears in the denominator in expression (32) for M and cannot be set equal to zero. Whereas Wright and Ockendon [16] considered strain-rate hardening, expression (35) for the shear band spacing is for non-strain-rate hardening materials. For such materials, $L_{WO} = 0$. However, we get a non-zero value of the shear band spacing. Whereas $L_{WO} \propto k^{1/4}$, in expression (35), $L_s \propto k$. Numerical results given in the next section provide an explanation for these differences. The approximate expressions, given in the Introduction, for the shear band spacing, L_{BC} , derived by Batra and Chen [12], and Chen and Batra [21] are for locally adiabatic deformations. Molinari [17] assumed that the strain-hardening parameter is small, expanded different quantities in terms

of this parameter, and retained terms of degree one in this parameter. We compare below the presently computed shear band spacing with that obtained from Molinari's asymptotic solution, and also delineate the effect of different material parameters on the shear band spacing.

As is done in buckling problems one can account for the specimen thickness, h , by assigning an integer value to \tilde{m} in Eqs. (10) or (11) so that $\tilde{\xi}$ is closest to $\tilde{\xi}_m$. This value of $\tilde{\xi}$ will give the shear band spacing.

5. Computation and discussion of results

5.1. Comparison of exact shear band spacing with Molinari's asymptotic solution

We first compare results computed from Eqs. (24) and (30) with those obtained from the asymptotic expression of Molinari [17] and employ the constitutive relation given in the Introduction with material parameters assigned following values:

$$\begin{aligned} m &= 0.019, \quad \nu = -0.38, \quad \mu_0 = 3.579 \text{ GPa}, \\ \rho &= 7800 \text{ kg/m}^3, \quad c = 500 \text{ J/kg K}, \\ k &= 50 \text{ W/m K}, \quad \beta = 0.9, \quad \gamma_i = 0.01, \\ \theta_i &= 300 \text{ K}, \quad \dot{\gamma}_0 = 10^4 \text{ s}^{-1}, \quad n = 0.107. \end{aligned} \quad (39)$$

Recall that Molinari's asymptotic solution is valid for $n \ll 1$; therefore the present results can be compared with his only for small values of n . For $n = 0.015$ and 0.035 , the two sets of results are depicted in Fig. 1. These reveal that if the homogeneous solution corresponding to a larger value of the shear strain is perturbed then Molinari's asymptotic solution for the shear band spacing matches well with the present exact solution. However, the two differ somewhat if the homogeneous solution at lower values of the shear strain is perturbed. For a shear strain of nearly 1 in an ASB, both techniques predict a shear band spacing of 1.3 mm for $n = 0.035$ and about

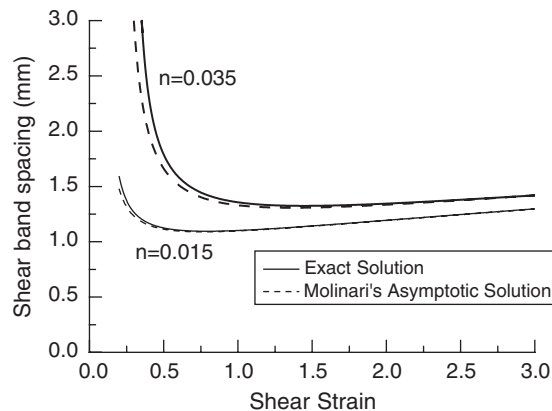


Fig. 1. For $n = 0.015$ and 0.035 , comparison of the shear band spacing computed from the present exact solution with that obtained from Molinari's asymptotic solution.

1.1 mm for $n = 0.015$ which are close to the experimental value of 1 mm observed by Nesterenko et al. [22]. For various values of the strain-hardening exponent n , we have plotted in Fig. 2 the variation of the relative difference, δ , defined by

$$\delta = |L_M - L_{BW}|/L_{BW} \tag{40}$$

with the shear strain at the instant of perturbing a homogeneous solution. Here L_{BW} denotes the shear band spacing computed from the present exact solution. It is clear from these plots that the difference between the two solutions increases with an increase in the value of the strain-hardening exponent n , and this difference is more pronounced at lower values of the shear strain.

5.2. Effect of different parameters on shear band spacing

We use the following constitutive relation:

$$\sigma = \sigma_0 \left(1 + \frac{\varepsilon}{\varepsilon_y}\right)^n (1 + b\dot{\varepsilon})^m \left(\frac{\theta_m - \theta}{\theta_m - \theta_0}\right)^v \tag{41}$$

for studying the effect of different parameters on the shear band spacing. For homogeneous deformations of a thermoviscoplastic body deformed at a constant strain rate, one needs the temperature as a function of strain. Prior to perturbing the homogeneous solution, the temperature is uniform in the body and there is no heat conduction except when the temperature is assigned at the boundaries. Substituting from Eq. (41) into Eq. (3) and integrating the resulting equation, we obtain

$$\theta = \theta_m - (\theta_m - \theta_r) \exp\left\{-\frac{\beta\sigma_0\varepsilon_y(1 + b\dot{\varepsilon}_0)^m}{\rho c(\theta_m - \theta_r)(n + 1)} \left[\left(1 + \frac{\varepsilon}{\varepsilon_y}\right)^{n+1} - 1\right]\right\}, \quad v = 1,$$

$$\theta = \theta_m - \left\{(\theta_m - \theta_r)^{1-v} - \frac{\beta(1 - v)\sigma_0\varepsilon_y(1 + b\dot{\varepsilon}_0)^m}{\rho c(\theta_m - \theta_r)^v(1 + n)} \left[\left(1 + \frac{\varepsilon}{\varepsilon_y}\right)^{n+1} - 1\right]\right\}^{1/(1-v)} \quad \text{for } v \neq 1. \tag{42}$$

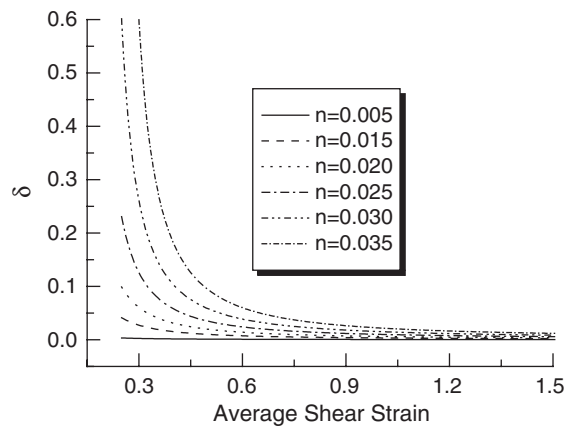


Fig. 2. For different values of the strain-hardening exponent n , dependence upon the average shear strain of the relative difference between the shear band spacings computed from the present solution and Molinari’s asymptotic solution.

Batra and Kim [24] determined values of material parameters appearing in Eq. (41) by solving an initial–boundary-value problem that closely simulated the experimental setup of Marchand and Duffy [25] and ensured that the computed stress–strain curve matched well with the test data. They obtained following values of parameters for HY-100 steel:

$$\begin{aligned} \sigma_0 &= 405 \text{ MPa}, \quad b = 17,320 \text{ s}^{-1}, \quad \rho = 7860 \text{ kg/m}^3, \quad k = 50 \text{ W/mK}, \quad n = 0.107, \quad m = 0.0117, \\ c &= 473 \text{ J/kgK}, \quad \varepsilon_y = 0.012, \quad \beta = 0.9, \quad \theta_m = 1500 \text{ K}, \quad \theta_0 = 300 \text{ K}, \quad \dot{\varepsilon}_0 = 3300 \text{ s}^{-1}, \quad \nu = 1. \end{aligned} \quad (43)$$

Because $b\dot{\varepsilon} \gg 1$ and $m \ll 1$, $(1 + b\dot{\varepsilon})^m \simeq b^m \dot{\varepsilon}^m$; thus m equals the strain-rate hardening exponent. Similarly for $\varepsilon \simeq 0.1$, $\varepsilon/\varepsilon_y \simeq 10$, and $(1 + \varepsilon/\varepsilon_y)^n \simeq (\varepsilon/\varepsilon_y)^n$. Fig. 3a–e illustrates the variation of the shear band spacing, based on Wright and Ockendon's definition, with the average strain when the homogeneous solution is perturbed for different values of thermal conductivity, nominal strain rate, strain- and strain-rate hardening and the thermal softening exponents. For a fixed value of the initial strain, the shear band spacing increases with an increase in the thermal conductivity, a decrease in the imposed strain rate, and a decrease in the thermal softening exponent ν . The trends are less clear for the effects of strain hardening and strain rate hardening exponents. Note that a large value of ν enhances the thermal softening effect. For initial shear strain greater than about 1.5, the shear band spacing increases with an increase in the strain-rate hardening exponent m . However, for the effect of strain-hardening exponent n , a clear trend emerges only when the initial shear strain exceeds about 3 in which case the shear band spacing decreases with an increase in n . This is rather unexpected. However, Eq. (37) provides an explanation. For $\varepsilon^0 \geq 3$, $1 + \varepsilon^0/\varepsilon_y \simeq (83.3\varepsilon^0)$ and with an increase in n this term decreases faster than $n^{1/4}$ resulting in a decrease in the value of L_s .

In order to elucidate further the variation of the shear band spacing L_s on the strain-hardening exponent n , we have plotted in Fig. 4a–c L_s vs. n for the Molinari, the Wright–Batra and the Johnson–Cook viscoplastic relations. Values assigned to different material parameters for the Wright–Batra relation are given in Eq. (43), for the Molinari relation in his paper, and for the Johnson–Cook [20] relation are for a typical steel. Whereas L_s increases monotonically with n for the Molinari relation, it decreases for the other two viscoplastic relations. With an increase in n , the maximum initial growth rate of the perturbation decreases for the Molinari relation, it increases for the other two viscoplastic relations. Thus the three viscoplastic relations give qualitatively different results which is consistent with Batra and Chen's [12] work who also scrutinized the Bodner–Partom relation.

Results in the Figures to follow are computed with Molinari's definition of shear band spacing and hence do not depend upon the strain when the homogeneous solution is perturbed. Fig. 5a–d depicts the variation of the shear band spacing with the nominal strain-rate, strain-rate-hardening exponent, strain-hardening exponent, and the thermal-softening exponent. It is clear that the shear band spacing monotonically increases with an increase in the strain-rate-hardening exponent but decreases essentially affinely with an increase in the strain-hardening exponent and the thermal-softening exponent. The dependence of the shear band spacing upon the nominal strain rate is discussed in detail below.

In an attempt to exhibit the rather strong coupling between the effects of the strain-rate hardening exponent m , and the thermal conductivity, we have plotted in Fig. 6a, on a log–log scale, the variation of the shear band spacing, L_{BW} , with the thermal conductivity for several

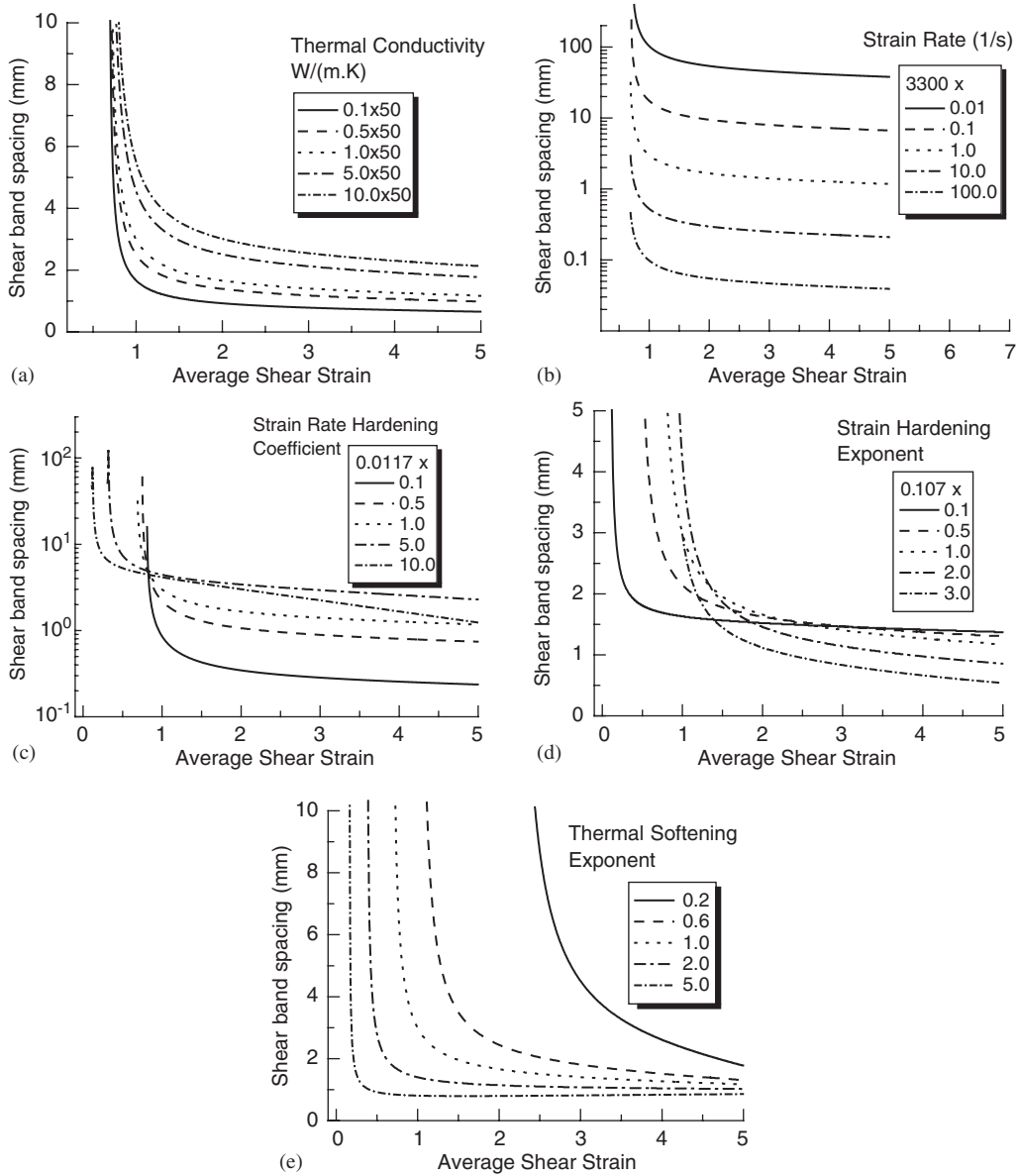


Fig. 3. For different values of material parameters, dependence of the shear band spacing upon the average shear strain when the homogeneous solution is perturbed.

values of m . For $m = 0$, the shear band spacing is finite as predicted by the Grady–Kipp expression but not by L_{WO} , L_{BC} and L_{CB} . For a fixed value of thermal conductivity (strain-hardening exponent), the L_{BW} increases with an increase in m (thermal conductivity). These plots suggest that

$$L_{BW} \propto k^\lambda, \tag{44}$$

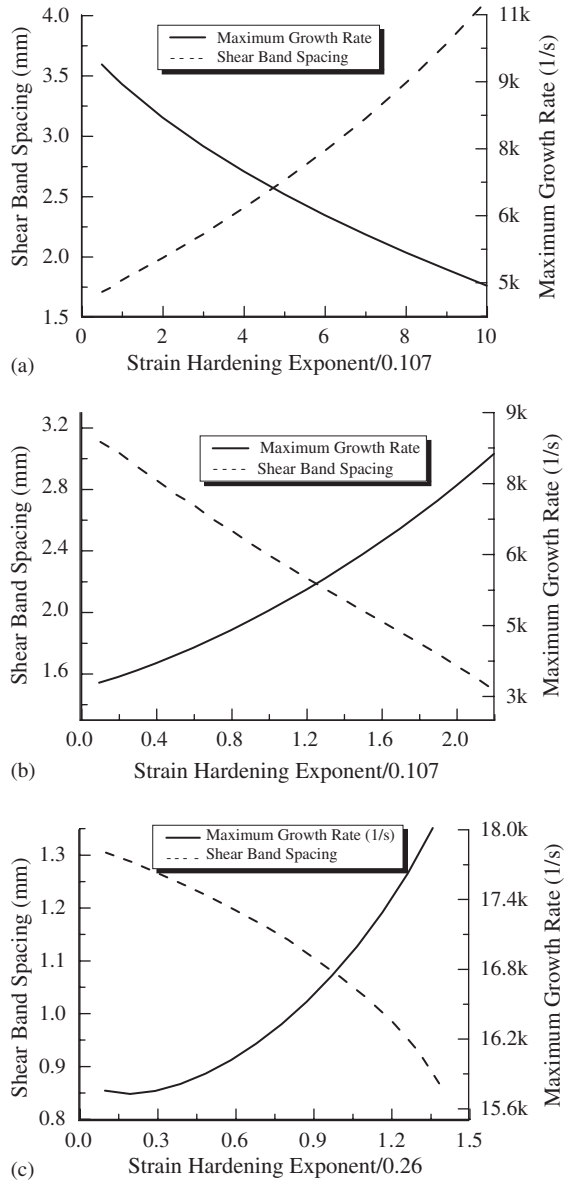


Fig. 4. Variation with n of the shear band spacing and the maximum initial growth rate of the perturbation for (a) Molinari's, (b) the Wright–Batra, and (c) the Johnson–Cook viscoplastic relations.

where the value of χ depends upon m ; this dependence is exhibited in Fig. 6b for two values of the strain-hardening exponent n . The value of χ does not vary much with n . For $m \geq 0.0001$, χ is almost 0.21 which is close to 0.25 appearing in the expressions for L_{WO} and \tilde{L}_{BC} . However, for $0 \leq m \leq 0.0001$, χ drops sharply from 1.0 at $m = 0$ to 0.21 at $m = 0.0001$. Batra and Chen [19] analyzed shear band spacing in strain-rate gradient-dependent materials. For the material

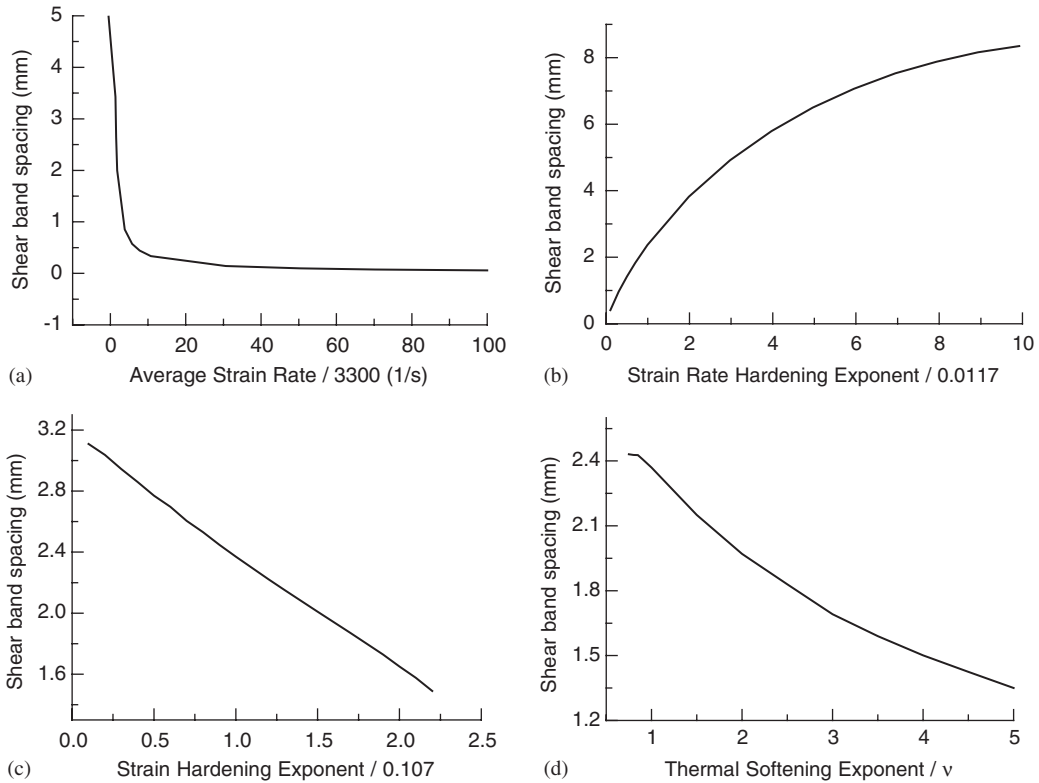


Fig. 5. Dependence of the shear band spacing computed with the definition $L = \inf_{f_0 \geq 0} (2\pi / \zeta_m(t_0))$ upon (a) the average strain rate, (b) strain-rate hardening exponent, (c) strain-hardening exponent, and (d) thermal-softening exponent.

behavior modeled by Molinari’s type viscoplastic relation, the shear band spacing ($= (0.76 + 0.0005k)$ mm, $10 \leq k \leq 220$ W/mK) increased affinely with an increase in the thermal conductivity k . However, when the material response was represented by the Wright–Batra relation (41), then the dependence of the shear band spacing upon k could be represented by Eq. (44); they did not determine χ .

The dependence of the shear band spacing upon the average strain rate, $\dot{\epsilon}_0$, is exhibited in Fig. 6c. It suggests that

$$L_{BW} \propto (\dot{\epsilon}_0)^{-0.787}. \tag{45}$$

The exponent -0.787 is close to -0.75 appearing in L_{WO} and \tilde{L}_{BC} but differs from -0.5 in L_{BC} and L_{CB} . Note that expressions for L_{BC} and L_{CB} are based on the assumption of locally adiabatic deformations, i.e., $k = 0$.

For different values of the strain-rate-hardening exponent m , we have plotted on a log–log scale the dependence of the shear band spacing L_{BW} upon the specific heat c in Fig. 7a. When written as

$$L_{BW} \propto c^{\chi_c}, \tag{46}$$

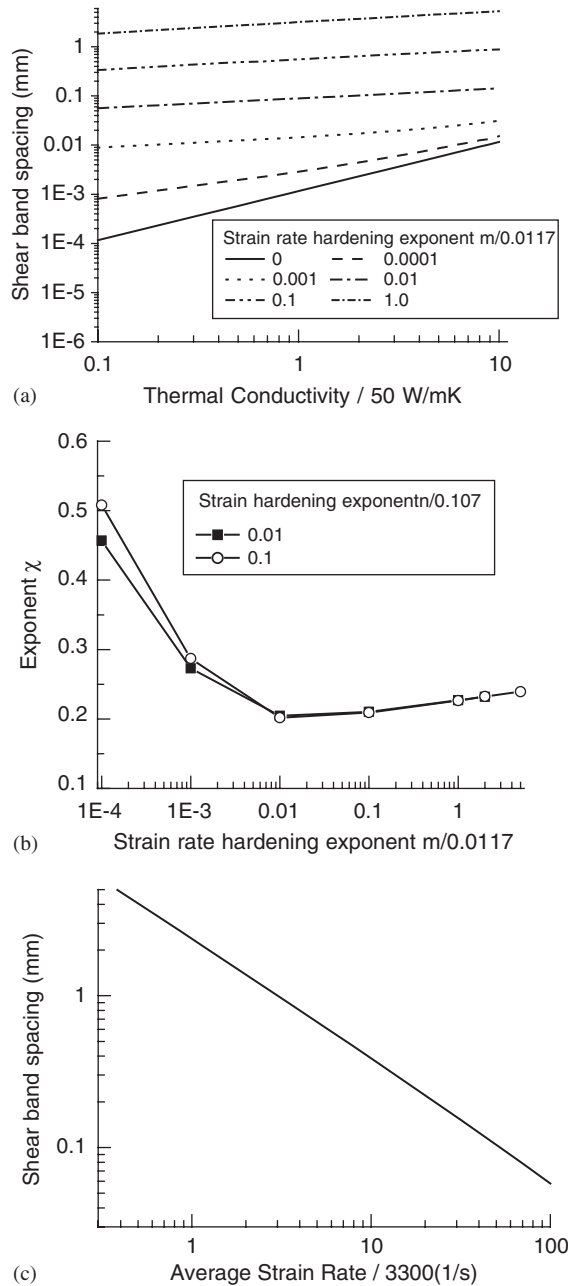


Fig. 6. (a) For different values of the strain-rate-hardening exponent m , variation of the shear band spacing with the thermal conductivity; (b) dependence of the exponent χ in Eq. (40) upon m ; (c) on a log-log plot, variation of the shear band spacing upon the average strain rate.

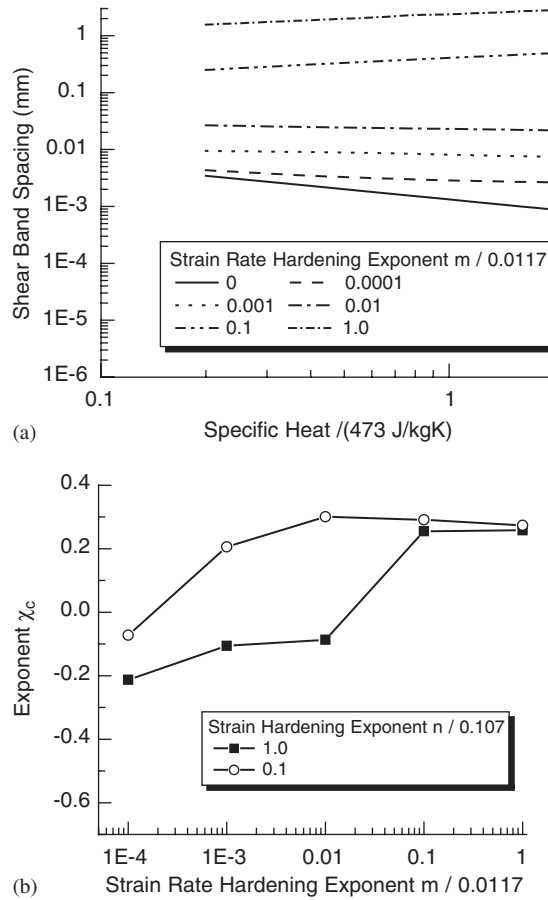


Fig. 7. (a) For different values of the strain-rate-hardening exponent m , dependence of the shear band spacing upon the specific heat; (b) variation of the scaling factor χ_c in Eq. (46) with m for $n = 0.0107$ and 0.107 .

χ_c depends upon m and n . The dependence of χ_c upon m and n is exhibited in Fig. 7b. $\chi_c = 0.274$ and 0.258 for $(m, n) = (0.0117, 0.107)$ and $(0.0117, 0.0107)$, respectively. However, for $m = 0$ and $n = 0.0107$ and 0.107 , $\chi_c = -0.596$ and -0.509 , respectively. Recall that for $n = 0$, $\chi_c = 0.25$ for L_{GK} , L_{WO} and L_M . Results depicted in Fig. 7b reveal that $\chi_c \approx 0.25$ only when $m \geq 0.1$ and $n = 0.0107$ or 0.107 . Our analysis shows that $\chi_c = 0.25$ is not valid for very weakly strain-rate-hardening materials.

For

$$L_{BW} \propto \beta^{\chi_\beta}, \tag{47}$$

Fig. 8a, b evinces the variation of L_{BW} with β for six values of m . It is clear that $\chi_\beta \approx -0.5$ for all values of m . Other investigators [16,12,21], except Molinari [17], set $\beta = 1$ and therefore did not delineate the influence of β upon the shear band spacing. Results plotted in Fig. 8b reveal that $-0.5 \leq \chi_\beta \leq -0.44$ for several combinations of the values of m and n , which is close to the value Molinari [17] obtained.

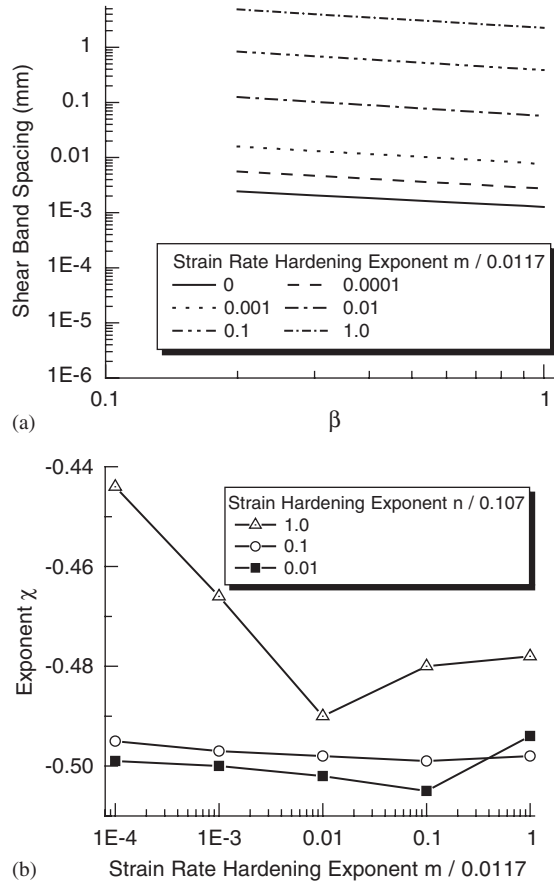


Fig. 8. For several values of the strain-rate-hardening exponent m , dependence of the shear band spacing upon the Taylor–Quinney parameter β ; (b) variation of the scaling parameter χ_β with m for three values of n .

The effect of the thermal-softening exponent ν upon the shear band spacing is exhibited in Fig. 9a and b. These plots reveal that the shear band spacing decreases monotonically with an increase in the value of ν . When the curve

$$L_{BW} = A \ln(\nu) + B \tag{48}$$

is fitted to the plots of Fig. 9a for $\nu \geq 1.5$ then following values of A and B are obtained (Table 1).

For the relation

$$L_{BW} \sim \nu^{\chi_\nu}, \tag{49}$$

the plots of Fig. 9b give

$$\chi_\nu = \begin{cases} -0.51 & \text{for } n = 0.0214, & 0.75 < \nu < 5, \\ -0.44 & \text{for } n = 0.0428, & 1 < \nu < 5. \end{cases} \tag{50}$$

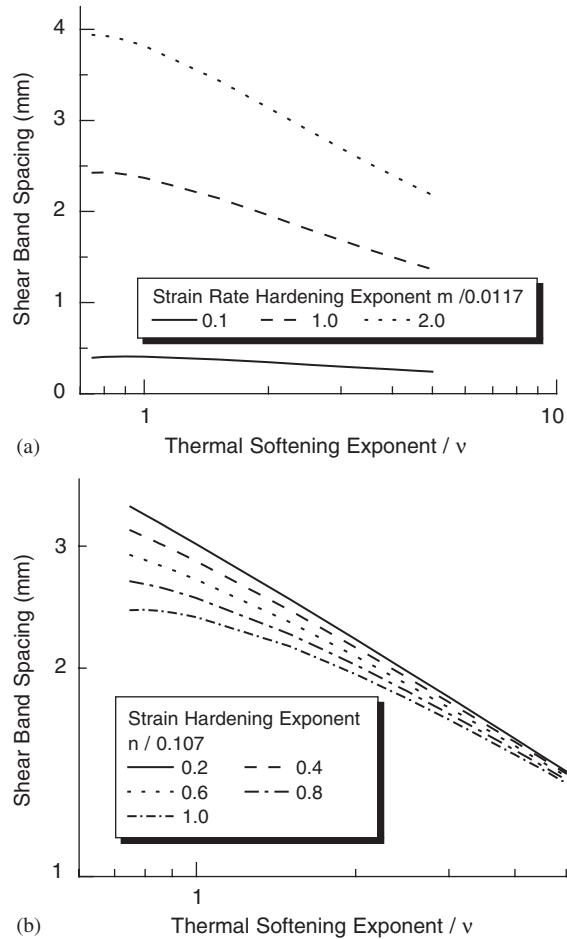


Fig. 9. For three values of the strain-rate-hardening exponent m and five values of the strain hardening exponent n , dependence of the shear band spacing upon the thermal-softening exponent v .

Table 1
Values of A and B in $L_{BW} = (A \ln(v) + B)$ mm

$m/0.0117$	0.1	1	2
A(mm)	-1.0177	-0.62521	-0.1026
B(mm)	3.8180	2.370	0.4071

5.3. Remarks

Because of the assumption that wavelengths considered are much smaller than the specimen thickness h , our results for the computed shear band spacing are valid for specimens at least a few cm thick. Otherwise only perturbations that vanish where velocity and temperature are prescribed

should be considered. In particular, shear band spacings computed by relations examined here are not valid for the experimental setup of Marchand and Duffy [25] since for specimens they tested $h = 2.58$ mm which is comparable to the computed shear band spacing. However, these analyses are valid for the explosively loaded cylinders tested by Nesterenko et al. [22].

We note that Batra and Chen [22], and Chen and Batra [29] have considered the effect of thermoviscoplastic relations and microstructural parameters on the shear band spacing. Batra [30] has delineated how different material parameters influence the shear band initiation.

6. Conclusions

We have used a perturbation method to analyze the stability of a homogeneous solution of equations governing coupled thermomechanical simple shearing deformations of a thermoviscoplastic body. By setting the shear band spacing equal to the wavelength of the perturbation having the maximum initial growth rate, we have found a closed-form expression for the shear band spacing. Results computed from it have been found to compare well with those obtained from Molinari's [17] asymptotic solution for small values of the strain-hardening exponent. It is found that the shear band spacing, L_{BW} , increases monotonically with an increase in the thermal conductivity k and the strain-rate hardening exponent m but decreases with an increase in the strain-hardening exponent n . When written as $L_{BW} \propto k^\chi$, the value of χ decreases from $\simeq 1.0$ at $m = 0$ to $\simeq 0.21$ at $m = 0.0001$. χ equals 0.23 when $m = 0.058$. Also, $L_{BW} \propto$ (nominal strain rate) $^{-0.787}$. The dependence of the shear band spacing upon the strain hardening exponent, the thermal-softening exponent, and the Taylor–Quinney parameter has also been characterized.

Acknowledgements

This work was partially supported by the US National Science Foundation grant CMS0002849, the ARO grant DAAD19-01-1-0657, and the ONR grants N00014-98-1-0300 and N00014-03-MP-2-0131 to Virginia Polytechnic Institute and State University. Partial support was also provided by the AFOSR MURI to Georgia Institute of Technology that awarded a subcontract to Virginia Tech. Z. G. Wei's work was also partially supported by the Chinese National Science Foundation grant 10002017. Views expressed in the paper are those of authors and not of funding agencies.

References

- [1] Tresca H. On further application of the flow of solids. Proc Inst Mech Eng 1978;30:301–45.
- [2] Zener C, Hollomon JH. Effect of strain rate upon plastic flow of steel. J Appl Phys 1944;14:22–32.
- [3] Bai YL. Thermo-plastic instability in simple shear. J Mech Phys Solids 1982;30:195–207.
- [4] Bai YL, Dodd B. Adiabatic shear localization, occurrence, theories, and applications. Oxford: Pergamon Press; 1992.
- [5] Wright TW. The physics and mathematics of adiabatic shear bands. Cambridge: Cambridge University Press; 2002.

- [6] Tomita Y. Simulation of plastic instabilities in solid mechanics. *Appl Mech Rev* 1994;47:171–205.
- [7] Zbib HM, Shawki T, Batra RC, editors. Material instabilities. *Appl Mech Rev* 1992;15:1–173 [special issue].
- [8] Armstrong R, Batra RC, Meyers M, Wright TW, editors. Shear instabilities and viscoplasticity theories. *Mech Mater* 1994;17:83–328 [special issue].
- [9] Perzyna P, editors. Localization and fracture phenomenon in inelastic solids, Wien, New York: Springer; 1998.
- [10] Batra RC, Zbib HM. Material instabilities: theory and applications. New York: ASME Press; 1994.
- [11] Batra RC, Rajapakse YDS, Rosakis A, editors. Failure mode transitions under dynamic loading. *Int J Fract* 2000;101:1–180 [special issue].
- [12] Batra RC, Chen L. Effect of viscoplastic relations on the instability strain, shear band initiation strain, the strain corresponding to the minimum shear band spacing, and the band width in a thermoviscoplastic material. *Int J Plasticity* 2001;17:1465–89.
- [13] Considère AG. Mémoire sur L'emploi du fer et de L'acier dans les constructions. *Annals des Ponts et Chaussées* 1885;9:574–775.
- [14] Batra RC, Kim CH. Effect of thermal conductivity on the initiation, growth and band width of adiabatic shear bands. *Int J Eng Sci* 1991;29:949–60.
- [15] Wei ZG, Batra RC. Dependence of instability strain upon damage in thermoviscoplastic materials. *Arch Mech* 2002;54:691–707.
- [16] Wright TW, Ockendon H. A scaling law for the effect of inertia on the formation of adiabatic shear bands. *Int J Plasticity* 1996;12:927–34.
- [17] Molinari A. Collective behavior and spacing of adiabatic shear bands. *J Mech Phys Solids* 1997;45:1551–75.
- [18] Grady DE, Kipp ME. The growth of unstable thermoplastic shear with application to steady-wave shock compression in solids. *J Mech Phys Solids* 1987;35:95–118.
- [19] Batra RC, Chen L. Shear band spacing in gradient-dependent thermoviscoplastic materials. *Comput Mech* 1999;23:8–19.
- [20] Johnson GR, Cook WH. A constitutive model and data for metals subjected to large strains, high strain-rates, and high temperatures. *Proceedings of the Seventh International Symposium on Ballistics*, 1983. p. 541–7.
- [21] Chen L, Batra RC. Effect of material parameters on shear band spacing in work-hardening gradient-dependent thermoviscoplastic materials. *Int J Plasticity* 1999;15:551–74.
- [22] Nesterenko VF, Meyers MA, Wright TW. Self-organization in the initiation of adiabatic shear bands. *Acta Mater* 1995;46:327–40.
- [23] Xue Q, Meyers MA, Nesterenko VF. Self-organization of shear bands in titanium and Ti-6Al-4V alloy. *Acta Mater* 2002;46:327–40.
- [24] Batra RC, Kim KH. Effect of viscoplastic flow rules on the initiation and growth of shear bands at high strain rates. *J Mech Phys Solids* 1990;38:859–74.
- [25] Marchand A, Duffy J. An experimental study of the formation process of adiabatic shear bands in a structural steel. *J Mech Phys Solids* 1988;36:251–83.
- [26] Batra RC. The initiation and growth of, and the interaction among adiabatic shear bands in simple and bipolar materials. *Int J Plasticity* 1987;3:75–89.
- [27] Batra RC, Kim CH. The interaction among adiabatic shear bands in simple and bipolar materials. *Int J Eng Sci* 1990;28:927–42.
- [28] Kwon YW, Batra RC. Effect of multiple initial imperfections on the initiation and growth of adiabatic shear bands in nonpolar and bipolar materials. *Int J Eng Sci* 1988;26:1177–87.
- [29] Chen L, Batra RC. Microstructural effects on shear instability and shear band spacing. *Theor Appl Fract Mech* 2000;34:155–66.
- [30] Batra RC. Effect of material parameters on the initiation and growth of adiabatic shear bands. *Int J Solids Struct* 1987;23:1435–46.